Hindawi
Shock and Vibration
Volume 2020, Article ID 8840051, 13 pages
https://doi.org/10.1155/2020/8840051

Research Article

Study on Microstructure Differences of Coal Samples before and after Loading

Jiajia Liu,[1,2,3] **Yingxiang Fang**,[2] **Gaini Jia**,[2] **Shouqi Chen**,[2] **and Jianmin Hu**[2]

[1]*State Collaborative Innovation Center of Coal Work Safety and Clean-Efficiency Utilization, Jiaozuo 454000, China*
[2]*School of Safety Science and Engineering, Henan Polytechnic University, Jiaozuo 454000, China*
[3]*State Key Laboratory Cultivation Base for Gas Geology and Gas Control, Henan Polytechnic University, Jiaozuo 454000, China*

Correspondence should be addressed to Jiajia Liu; liujiajia@hpu.edu.cn

Received 13 September 2020; Revised 7 October 2020; Accepted 29 October 2020; Published 30 November 2020

Academic Editor: Gang Zhou

The microscopic pore structure of coal affects the content of adsorbed gas. The microstructure of coal sample before and after loading is different, which will affect the adsorption and permeability of coal seam gas. In order to study this difference, the authors carried out mercury intrusion experiments on coal containing different coal samples and used nondestructive nuclear magnetic resonance (NMR) techniques, scanning electron microscopy, and transmission electron microscopy, to study the microstructure of coal samples before and after loading. The experimental results show that the pores of coal samples are mainly micropores and small pores, and the mesopores and macropores are relatively few. The T_2 spectrum area of the coal sample is significantly increased after loading, and the parallel-layer coal samples' T_2 spectrum area is 46735, which is 9112 more than the vertical layer coal samples. The T_2 spectrum of the vertical coalbed of saturated water samples shows a three-peak shape, the peak of the T_2 spectrum is 12692, and the parallel bedding shows a bimodal morphology. The peak area of the T_2 spectrum is 11277. The permeability of the parallel bedding coal sample is good, and the coal sample exhibits anisotropic properties. The pores and cracks of the coal samples increased after loading, and the localized area of the coal sample collapsed and formed a fracture zone, which was not conducive to the occurrence of coal seam gas. Further explanation of the changes in the permeability of the coal sample before and after loading will affect the gas storage and transportation.

1. Introduction

Mine gas disasters have always been a problem that plagues the safe production of the coal industry. Gas drainage for coal seams is an important technical means to control gas disasters, and mastering the gas storage and seepage characteristics in coal seams is essential for gas drainage design [1, 2].

Coal is a porous medium in which gas is present in the coal body in an adsorbed and free state and is present in minute pores. In the process of coal mining, the coal seam is affected by the coal mining machine, hydraulic fracturing, and other mining disturbances. The original equilibrium state of the coal seam is broken, the microstructure of the coal body changes, and the gas continuously desorbs from the coal and causes the coal to flow out, which leads to gas outburst accidents. At present, scholars at home and abroad have studied the microstructure of coal bodies before and after loading and the changes in physical properties of coal reservoirs. Direct observations have been made by scanning electron microscopy and transmission electron microscopy. The most commonly used qualitative analysis method is scanning electron microscopy [3, 4]. The mechanical behavior of coal samples after different pressurization and unloading modes [5–8] hydraulic fracturing can increase the permeability of coal seams by injecting high pressure into the cracks [9]. However, the effects of different axial pressures and confining pressures on permeability are different: the influence of axial pressure on permeability is less than confining pressure [10], gas pressure; under different confining pressures and full stress-strain conditions, the permeability decreases first and then increases [11, 12], which is consistent with the permeability results of the briquette and raw coal studied by the

scholars [13, 14] under triaxial stress. While the scholars [15] studied the triaxial compression state, the full stress-strain curve of the coal sample has a similar trend. The mechanism of deformation caused by deformation is different. The seepage velocity of briquette is most sensitive to axial force and axial deformation, while the seepage velocity of raw coal is sensitive to lateral deformation and volume deformation. Scholars [16] believe that the number of loadings/loads also affects the permeability of coal samples. Under repeated loading/unloading conditions, the stress (strain)-acoustic emission (coal rock fracture)-permeability (flow) changes are consistent and mutual omen. The reason why the permeability of coal is changed is related to the change of pore structure inside the coal body. Scholars [8, 17–19] found that the sudden increase of permeability of unloading coal is the result of the combination of primary fracture expansion and new fissure, simultaneous addition, and unloading [20]. Different degrees of coal have different degrees of damage expansion and permeability change. The coal body damage and penetration have synergistic evolution characteristics, but permeability change has hysteresis with respect to damage expansion [21, 22]. Scholars [23] have considered the triaxial seepage experiments carried out under high-pressure water and negative pressure loading conditions. As the confining pressure increases, the permeability of coal samples before fracturing decreases then decreases and then increases after fracturing. China's coal seam occurrence environment is complex; the coal layer's bedding structure will also affect the permeability of coal samples [24–26]. Scholars [27] through scanning electron microscopy to highlight the coal seam parallel layer and vertical bedding microporosity and the microfracture observation found that the coal sample structure was not uniform, and it was mainly composed of granular, reticular, and flaky structures. The transient permeability test showed that the permeability of coal samples was not obvious. The particle size of coal sample after loading and crushing also has an effect on permeability: scholars [28, 29] separately considered the permeability change of coal samples with different particle sizes under load and found that the permeability coefficient and compaction of broken coal bodies with different particle sizes were observed. Closely related, the permeability coefficient decreases with the increase of axial pressure. The mesostructure experiment of the permeability change caused by the coal sample after loading: CT scanning, infrared spectroscopy, etc., in which the scholar [30] studied the CT scan of the test piece before and after the coal penetration test under the full stress-strain condition and found that the through crack occurred. It was produced after the infiltration experiment. Scholars [31] used X-ray microcomputed tomography to detect the closure of trace elements in coal caused by effective stress, resulting in a sharp drop in permeability, but only a modest decrease in porosity. Scholars [32] conducted a comparative analysis of the infrared spectra and transmission electron microscopy results of coal samples before and after unloading. The effects of loading and unloading on the permeability characteristics and the microstructure changes of coal bodies were discussed from a microscopic point of view. Scholars [33–35] used mercury intrusion to test the microstructure of coal. In TDC, pores and cracks developed strongly, gas seepage channels were clear, and the permeability of TDC was much greater than that of undeformed coal.

In summary, domestic and foreign scholars have studied the pore structure of coal caused by different loading modes and then studied the influence of coal permeability and the relationship between coal microstructure change and permeability and effective porosity. Some experimental instruments are not comprehensive enough to observe the microstructural scale of coal, and the instrument will cause damage to the coal body and only stay in qualitative analysis. Therefore, the author uses the nondestructive nuclear magnetic resonance (NMR) technology, scanning electron microscopy (SEM), and transmission electron microscopy (TEM) to study the microstructure changes before and after the loading of the coal body and the relationship between the change and the permeability and the effective porosity, in order to grasp the coal microstructure change before and after the loading of the coal body and the impact of the gas storage and transportation.

2. Pore Distribution and Basic Physical Parameters of Coal

2.1. Pore Distribution of Coal. The specific surface area is an important parameter reflecting the pore structure of the coal, and the porosity is the main factor determining the permeability of the coal. At present, the mercury intrusion method is commonly used to determine the pore structure of coal. The principle is that the mercury enters the solid by pressurization, and the energy required to increase the pore volume into the solid pore is equal to the work done by the external force, which is equal to the same thermodynamic condition surface free energy at the mercury-solid interface. The instrument used in the experiment is the AutoPore IV 9500 mercury intrusion meter. It has three modes of operation: fast scanning, time, or rate balancing and has higher precision data acquisition. The test results of AutoPore IV 9500 mercury intrusion meter are shown in Figures 1 and 2.

It can be seen from Figures 1 and 2 and Table 1 that the specific surface area of the coal pores (<10 nm) accounts for 71.9% of the total specific surface area, and the specific surface area of the coal pores (10–100 nm) accounts for 27.8% of the total specific surface area. The specific surface area of the pores (100–1000 nm) accounts for 0.276% of the total specific surface area, and the specific surface area of the coal pores (>1000 nm) accounts for 0.046% of the total specific surface area. The pores and macropores of the coal body account for the total specific surface area. The ratio is minimal. The experimental results of mercury intrusion technology show that the pores of coal body are mainly micropores and small pores, and the mesopores and macropores are relatively few.

2.2. Coal Sample Basic Parameters and Industrial Analysis. According to the coal sample industry analysis and determination standard GB/T212-2006, firstly, the coal sample is crushed and sieved with a 0.2 mm particle size standard sieve

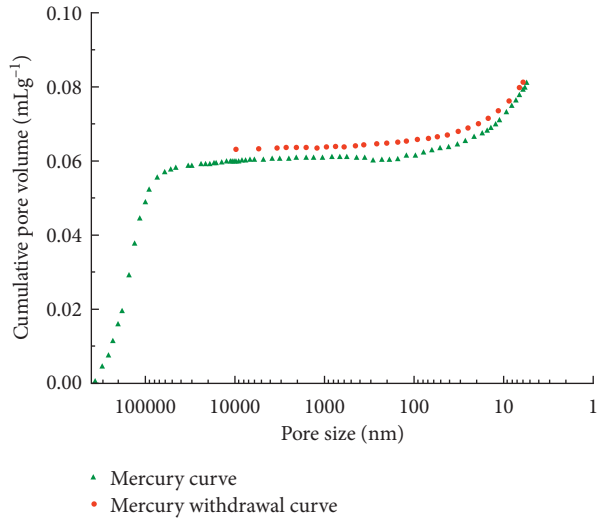

Figure 1: Experimental curves of cumulative pore volume with pore.

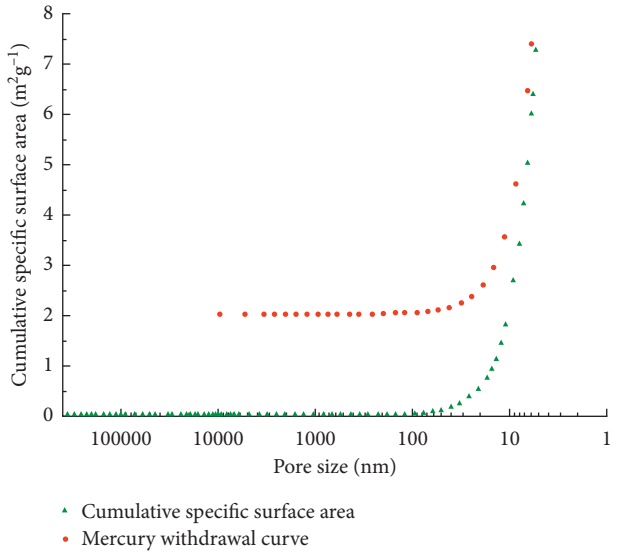

Figure 2: Accumulation of specific surface area with pore diameter.

to take about 1 g coal sample, and the 5E-MAG6600 automatic industrial analyzer is used for coal sample industrial analysis and test. The specific coal sample industry analysis test results are shown in Table 2.

It can be seen from Table 2 that the coal content of the coal used in the experiment is 0.83%, the ash content is 10.02%, the volatile content is 18.19%, the ultimate adsorption constant a is 39.02 m^3/t, and the adsorption constant b is 0.329 MPa^{-1}

The coal sample was uniaxially pressurized, and after 12 hours of water saturation, the T_2 spectrum of the coal sample was measured by NMR technique. It can be seen from Figures 3 and 4 that the T_2 spectrum area of the coal sample is significantly increased after loading, and the parallel-layer coal sample T_2 spectrum area is 46735, which is 9112 more than the vertical layer coal sample. The first peak area of the microscopic pores in the parallel bedding accounts for 57.6% of the total area, and the vertical bedding was 66.4%. The third peak area for characterizing macropores and fissures in parallel bedding accounts for 38.2% of the total area and 27.5% for the vertical. The difference in T_2 spectral area of coal samples with the same loading conditions is mainly due to the difference in bedding. Under the loading conditions, the pore and fracture area of the coal sample increased significantly, indicating that the gas migration channel of the coal sample was unblocked.

3. Low Field NMR Experimental Test

In recent years, NMR technology has been favored by scholars at home and abroad for its rapid, nondestructive, and visual technical advantages and has become a new method for studying the pore characteristics of coal bodies. It is based on the principle that the hydrogen nuclei will be aligned under the action of an external magnetic field to measure the relaxation characteristics of the hydrogen-containing nuclear fluid (water) in the pores of the coal rock and obtain the nuclear magnetic resonance intensity and the transverse relaxation time T_2. The relationship curve is obtained to obtain the pore fracture distribution characteristics of the coal sample. According to the principle of NMR technology, the T_2 spectrum reflects the amount and distribution of pores in the coal sample. The area of the closed pattern enclosed by the T_2 spectrum and the x-axis, referred to as the T_2 spectrum area, represents the volume of pores in the coal sample; T_2. The pattern change of the spectrum reflects the distribution of the pore size in the coal sample. The larger the T_2 is, the larger the pore size is. The smaller the pore size is, the closer the T_2 spectrum is to the left and the larger the proportion of the tiny pores of the coal sample. This achieves a fine quantitative characterization of microstructures in coal using low field NMR methods [36–39]. After the coal sample is saturated and centrifuged, the core is tested and analyzed by NMR technology to obtain the nuclear magnetic porosity, effective porosity, and direct permeability of the coal sample.

It can be clearly seen from Figures 5 and 6 that the $T2$ spectral areas of coal samples are different under different water conditions, and the order is T_2 spectral area of the coal sample after drying (2040 dimensionless) < T_2 spectral area of coal sample under natural water condition (3080) < T_2 spectral area of saturated coal samples (11984). The T_2 spectrum of the vertical bedding in different water conditions is larger than that of the parallel bedding. The T_2 spectrum of the vertical coalbed of saturated water samples shows a three-peak shape, the peak of the T_2 spectrum is 12692, and the parallel bedding shows a bimodal morphology. The peak area of the T_2 spectrum is 11277, and the coal sample exhibits anisotropic characteristics in the bedding. The area of the T_2 spectrum decreases from natural to dry, indicating that the moisture in the coal evaporates continuously from the micropores in dry conditions and is lost along the pore channels. The area of T_2 spectrum increased after the dry coal sample was

Table 1: Pore distribution of coal.

Pore classification	Microporous	Small pore	Mesopore	Macropore	Total mercury intake (mL/g)	Mercury withdrawal (mL/g)	Porosity (%)
	<10 nm	10–100 nm	100–1000 nm	>1000 nm			
Specific surface area m^2/g	4.69	1.81	0.018	0.003	0.0811	0.063	9.18
	71.9%	27.8	0.276%	0.046%			

Table 2: Basic physical parameters of coal.

Moisture (%)	Ash (%)	Volatile (%)	Adsorption constant	Adsorption constant
0.83	10.02	18.19	a (m^3/t)	b (MPa^{-1})
			39.02	0.329

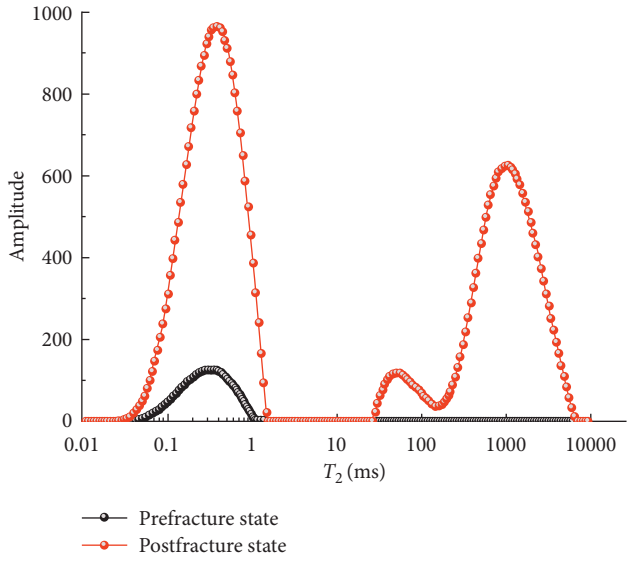

Figure 3: T_2 distribution of parallel layers at different water conditions of Yuwu, Shanxi.

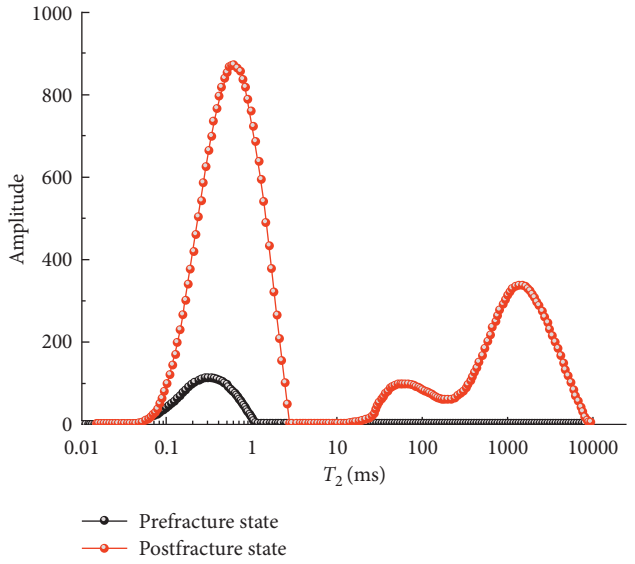

Figure 4: T_2 distribution of vertical bedding at different water conditions of Yuwu, Shanxi.

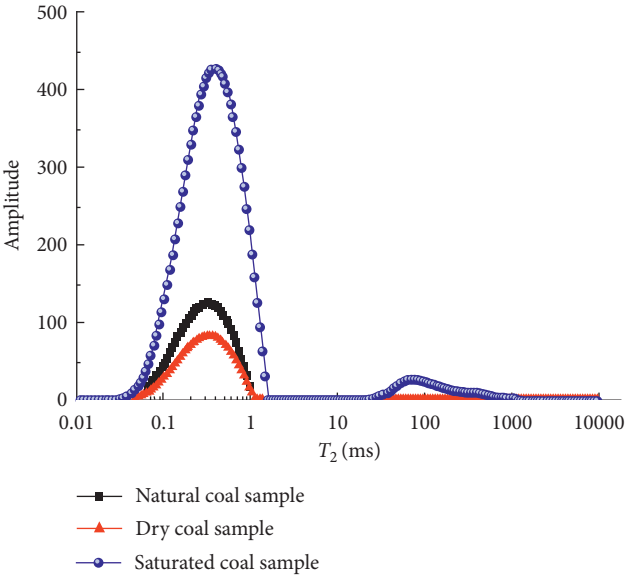

Figure 5: T_2 distribution and porosity distribution of parallel layers at different water conditions.

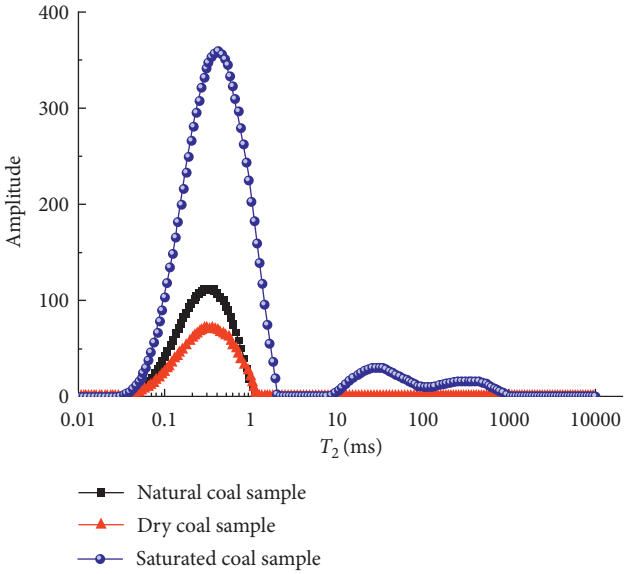

Figure 6: T_2 distribution and porosity distribution of vertical bedding at different water conditions.

saturated, indicating that the water entered the coal pores and the mesopores from the coal fissure channel and then entered the micropores. The above experimental results show that the connectivity between the pores in the coal is good as a whole.

It can be seen from Figures 7 and 8 that after the centrifugal coal sample is centrifuged, the T_2 spectral area is significantly reduced, and the moisture in the coal sample is extracted from the coal pores under the action of centrifugal force. The results of nuclear magnetic resonance measurement results show that the nuclear magnetic porosity of the parallel coal sample is 3.906%, and the nuclear magnetic porosity after centrifugation is 1.192%. The difference between the two is 2.714%. The nuclear magnetic porosity of the vertical bedding coal sample is 3.856%, and the nuclear magnetic porosity after centrifugation is 1.295%. The difference between the two is 2.561%. The greater the effective porosity, the better the permeability of the coal sample and the better communication between the internal layers of the coal sample. This is also seen from the number of pores and the continuity between the peaks. The experimental results also show that the layered structure has an influence on the permeability of coal samples. The fluid is infiltrated by the laminar flow in the parallel-layer coal sample, and the layered fissure communication condition is good, while the vertical bedding is good. On the contrary, the bedding fissures have poor communication conditions in the direction of seepage, and the permeation resistance is large.

4. Coal Body before and after the Loading Scanning Electron Microscope Test

The experimental coal samples were taken from the 29031 working face of a mine, and the coal type is high metamorphic lean coal. The CamScan MX2600 thermal field emission scanning electron microscope was used to test the microscale before and after the coal samples were loaded. It is necessary to pay attention to the sample after the load is the true three-axis loaded coal body seepage characteristics test after the failure of the coal sample, in order to avoid coal samples. For the discreteness of the scanning results, try to use a cubic coal sample with a complete appearance of a small size of about 0.5 cm^3, and select a relatively flat section as the observation surface for observation. The CamScan MX2600 thermal field emission scanning electron microscope is shown in Figure 9. The specific SEM test results are shown in Figure 10.

It can be seen from the analysis of Figure 10 that the structure of the coal body is dense and the surface is rough. There are many hollow holes of different sizes and irregular shapes, but there is no obvious crack in the coal body before loading, which is not conducive to the coal body gas seepage. After the coal body was loaded, its dense structure was destroyed, a large number of fissures were formed, and the original pores were further connected. A large number of shear fissures were observed, which greatly increased the permeability of the coal body.

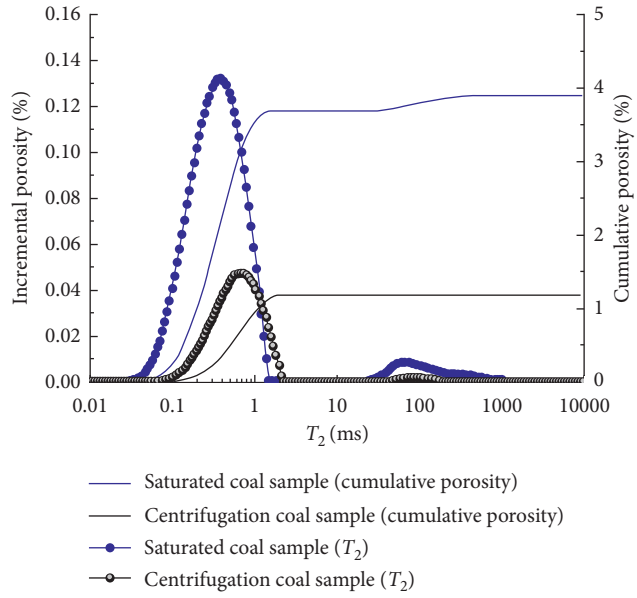

Figure 7: T_2 distribution and porosity distribution of parallel layers at saturated and centrifugal conditions.

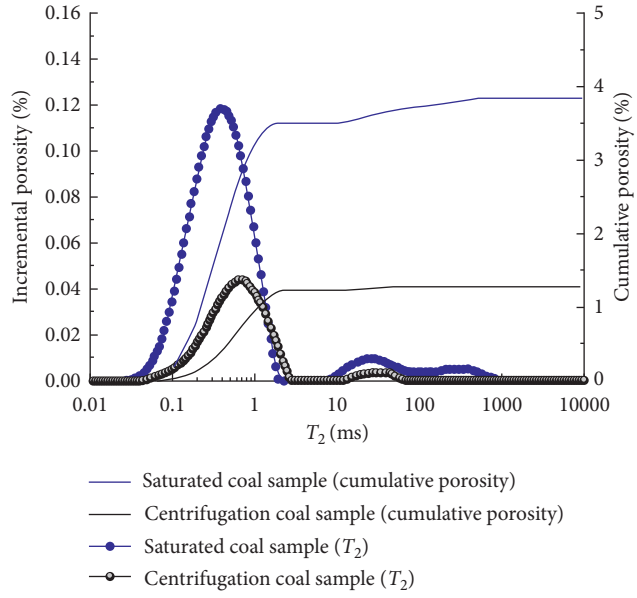

Figure 8: T_2 distribution and porosity distribution of vertical bedding at saturated and centrifugal conditions.

5. Before and after the Load of Coal by Transmission Electron Microscopy

In order to grasp the changes of the internal microstructure of the coal before and after loading and the penetration and expansion characteristics of the crack, a high-resolution transmission electron microscope of the Japanese model JEM-2100 was used to test the morphology and microstructure of the coal before and after loading. From the microscopic angle, the influence of the internal microstructure on the seepage characteristics is further analyzed. It is necessary to pay attention to the sample after the load is

Figure 9: CamScan MX2600-type thermal field emission scanning electron microscopy.

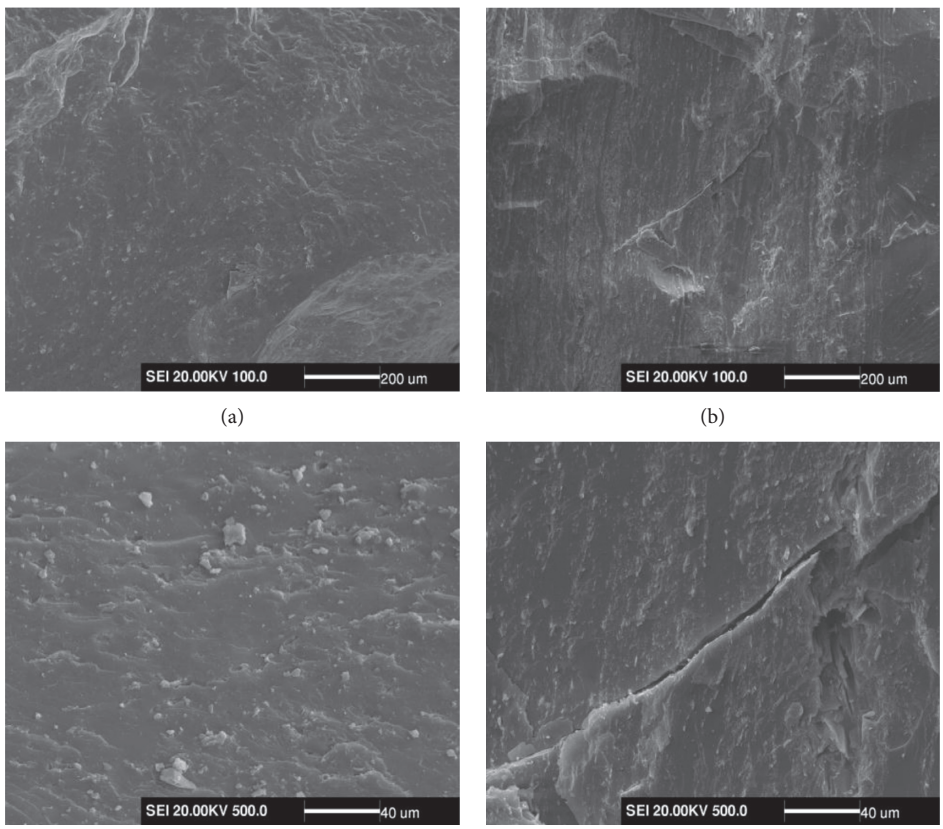

(a) (b)

(c) (d)

Figure 10: Continued.

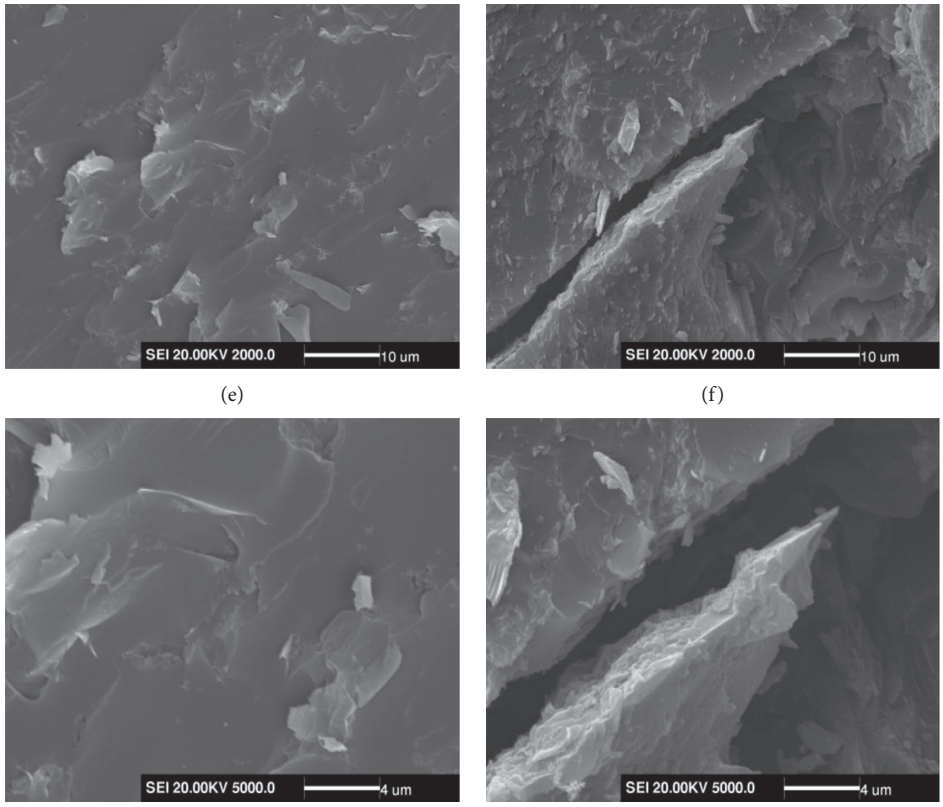

Figure 10: Scanning electron micrograph of coal body before and after loading. (a) Before loading100 (100 times). (b) After loading (100 times). (c) Before loading (500 times). (d) After loading (500 times). (e) Before loading (2000 times). (f) After loading (2000 times). (g) Before loading (5000 times). (h) After loading (5000 times).

the coal sample after the failure of the seepage characteristics of the true triaxial loaded coal.

The high-resolution transmission electron microscope (JEM-2100) has a test magnification of 2 to 800,000 times. The physical diagram of the specific equipment is shown in Figure 11.

High-resolution transmission electron microscopy tests the internal microstructure and morphology of the coal body before loading. As shown in Figure 12, it can be seen from the analysis of Figure 12 that the microstructure of the coal sample before loading is smooth, and the outer edge of the coal particles is smooth too The end face is also relatively complete. By analyzing the original coal body before loading, it is known that the microstructure in the original coal body is not conducive to the circulation of gas in the coal body.

The internal microstructure of the coal after loading is shown in Figure 13. It can be seen from the analysis of Figure 13 that after the coal body is damaged by the load, obvious pores and cracks appear, and the local area collapses and forms a crushing zone. The outer edges of the coal particles are irregular and uneven, and the surface of the coal body is weakened and in the coal powder area, the traces of gas flow are clearly seen.

Figure 11: JEM-2100-type transmission electron microscope.

Further analysis of the microstructure at 50 nm and 20 nm in Figures 13(d) and 13(e) reveals a main fracture of the coal body. A large number of secondary fractures appear around the main fracture. The main fracture and the secondary fracture all develop along the same direction. It is relatively developed and has obvious fractal characteristics.

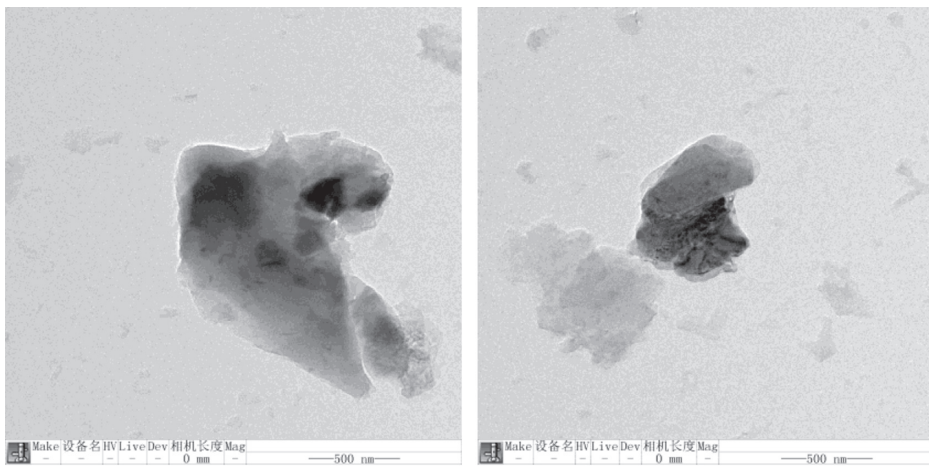

(a)

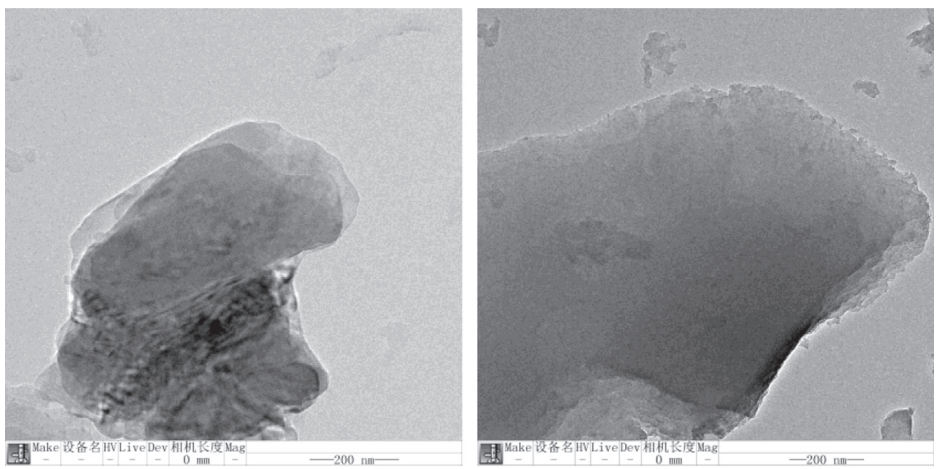

(b)

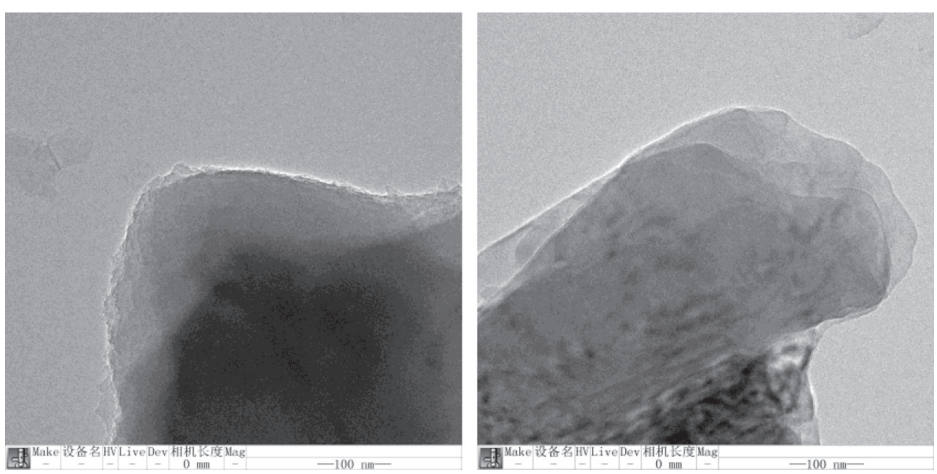

(c)

Figure 12: Continued.

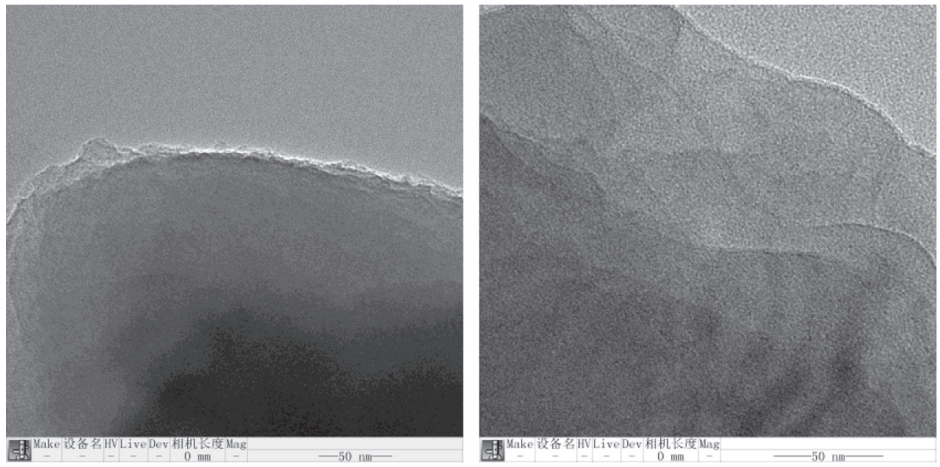

(d)

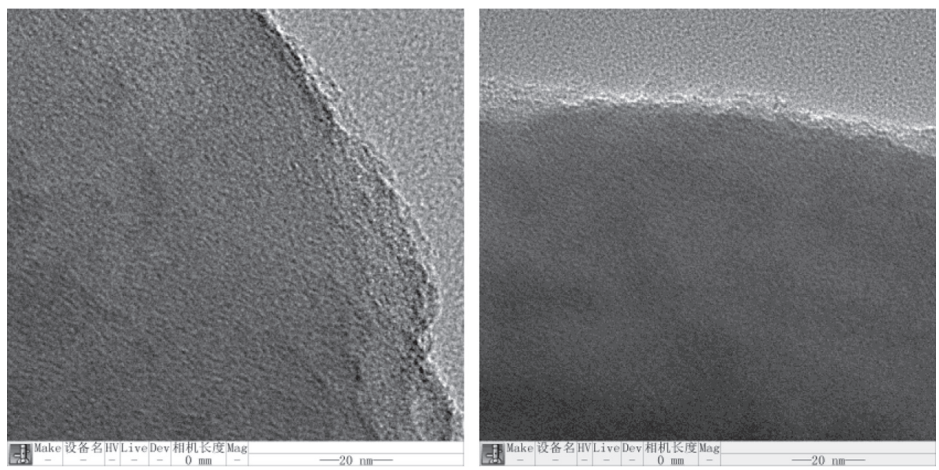

(e)

Figure 12: Microstructure and morphology of coal body before loading. (a) 500 nm. (b) 200 nm. (c) 100 nm. (d) 50 nm. (e) 20 nm.

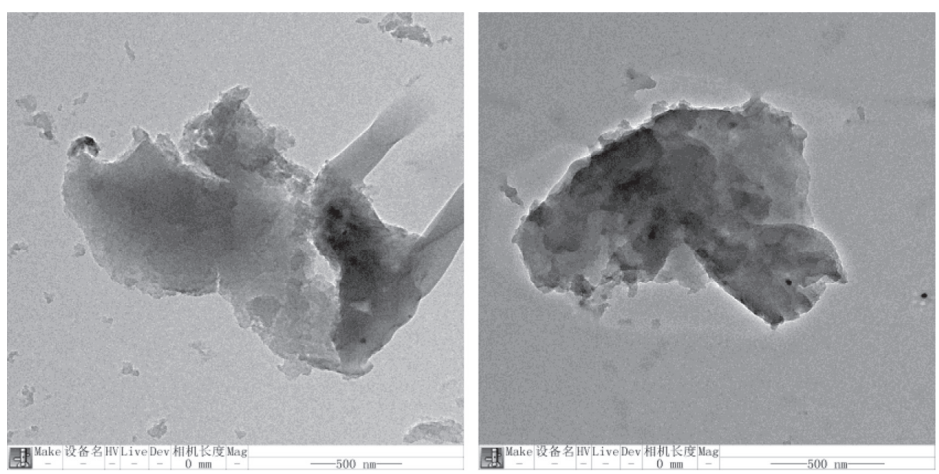

(a)

Figure 13: Continued.

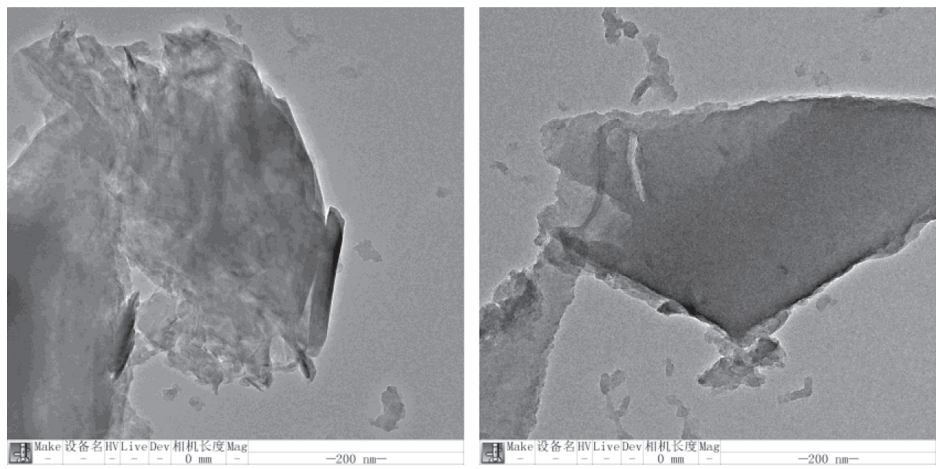

(b)

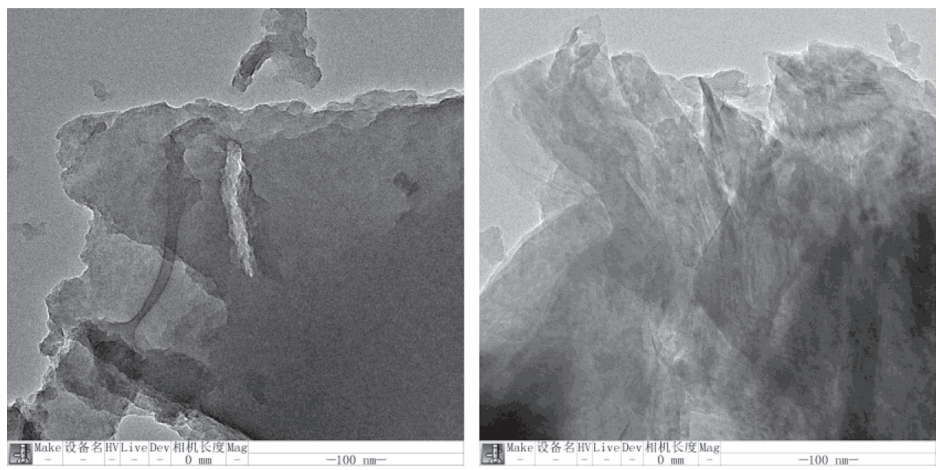

(c)

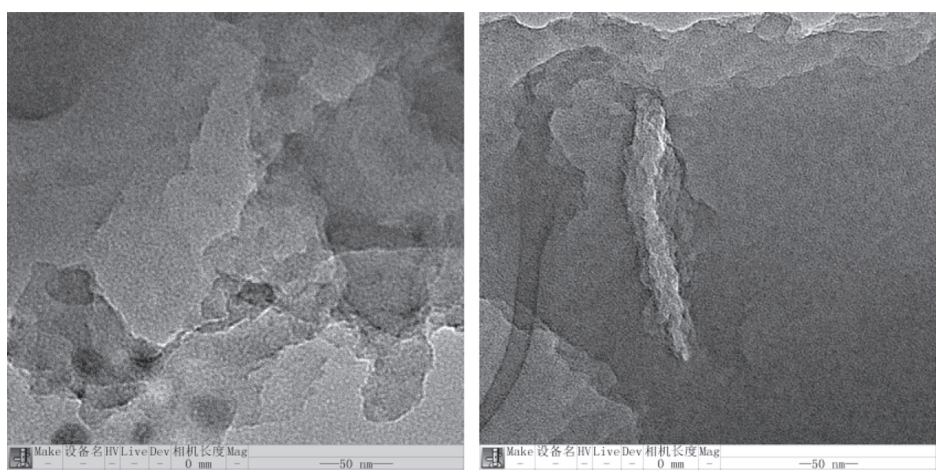

(d)

Figure 13: Continued.

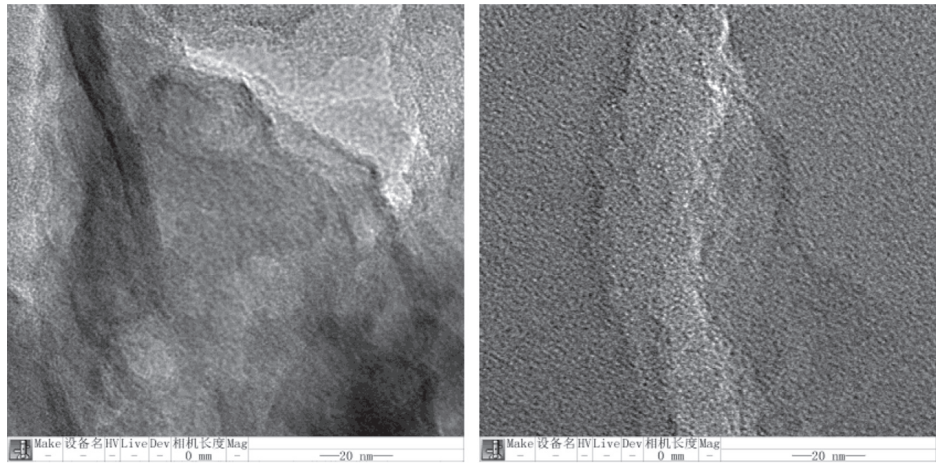

(e)

Figure 13: Microstructure and morphology of coal after loading. (a) 500 nm. (b) 200 nm. (c) 100 nm. (d) 50 nm. (e) 20 nm.

The tip of the fracture also has divergent characteristics. These fractures are the origin of microcracks and pore development and are also gas seepage, diffusion channels, and enrichment zones. Through the high-resolution projection electron microscopy analysis of the internal microstructure of the coal before and after loading, it can be seen that the number of pores and cracks of the coal body after the load is damaged is obviously increased, which is beneficial to the expansion, development, and penetration of the crack, and finally in the coal body, the seepage characteristics are significantly increased.

6. Conclusions

(1) In the mercury intrusion test, the pores of the coal body are mainly micropores and small pores, and the mesopores and macropores are relatively few. The T_2 relaxation time of the coal pores obtained by NMR test is mainly in the 0.1~1 ms region. The parallel layer of the coal sample under natural, dry, and saturated conditions has a larger T_2 spectrum than the vertical bedding, and the coal sample exhibits anisotropic properties. The effective porosity of the coal sample affects the permeability of the coal sample.

(2) The microscale test of the coal body before and after loading was carried out by scanning electron microscopy. After the coal body was loaded, its dense structure was destroyed, a large number of cracks were formed, and the original pores were further penetrated, which further increased the permeability of the coal body.

(3) High-resolution transmission electron microscopy was used to test the internal microstructure changes of coal before and after loading. After the coal was loaded, obvious pores and fissures appeared, the weakened coal powder area appears on the surface of the coal body, the local area collapses and forms a fracture zone, and the gas flow traces can be clearly seen. The increase of cracks is conducive to the expansion and penetration of cracks and improves the permeability of coal.

Data Availability

The data used to support the findings of this study are included within the article.

Disclosure

This work was presented at the Mine Ventilation Conference 2019, as a very short abstract in a poster.

Conflicts of Interest

The authors declare that they have no conflicts of interest regarding the publication of this paper.

Acknowledgments

This work was supported by the National Natural Science Foundation of China (nos. 52074106, 51734007, and 51704099). This project was also supported by Zhongyuan Postdoctoral Innovative Talent (ZYQR201810171), the National Key Research and Development Program of China (2018YFC0808103), the China Postdoctoral Science Foundation (Grant no. 2019M652536), the Henan Postdoctoral Foundation (001801016), and the Key R&D and Promotion Special Projects of Henan Province (192102310511) and funded by the Doctoral Fund of Henan Polytechnic University (no.B2018-59).

References

[1] P. Zhao, R. Zhuo, S. Li et al., "Analysis of advancing speed effect in gas safety extraction channels and pressure-relief gas extraction," *Fuel*, vol. 265, Article ID 116825, 2020.

[2] P. X. Zhao, R. S. Zhuo, S. G. Li et al., "Fractal characteristics of gas migration channels at different mining heights," *Fuel*, vol. 271, pp. 169–171, 2020.

[3] M. Wang and Y. W. Wang, "SEM analysis of coal microstructure in pingdianshan mining area," *Coal Safety*, vol. 30, no. 7, pp. 169–171, 2014.

[4] M. M. Li, *The Research on Pyrolysis-Penteation and Microstructure of Lignite*, Taiyuan University of Technology, Taiyun, china, 2012.

[5] Q. C. Fu, *Creep-Seepage Law and Microscopic Response Characteristics of Coal Containing Gas*, Henan Polytechnic University, Jiauzuo, China, 2016.

[6] L. Meng, *Research on Coal Damage Characteristics and Gas Migration Law of Coal Containing Gas*, China University of Mining and Technology, Beijing, China, 2013.

[7] K. H. S. M. Sampath, M. S. A. Perera, D. Elsworth, P. G. Ranjith, S. K. Matthai, and T. Rathnaweera, "Experimental investigation on the mechanical behavior of victorian Brown coal under brine saturation," *Energy and Fuels*, vol. 32, no. 5, pp. 5799–5811, 2018.

[8] W. Z. Du, Y. S. Zhang, X. B. Meng, X. Y. Zhang, and W. X. Li, "Deformation and seepage characteristics of gas-containing coal under true triaxial stress," *Arabian Journal of Geosciences*, vol. 11, no. 9, pp. 1–13, 2018.

[9] T. Wang, W. Zhou, J. Chen, X. Xiao, Y. Li, and X. Zhao, "Simulation of hydraulic fracturing using particle flow method and application in a coal mine," *International Journal of Coal Geology*, vol. 121, pp. 1–13, 2014.

[10] D. Qu, X. Li, J. Zhang, D. Li, and G. Wang, "Study on the characteristics of gas permeability of coal under loaded stress," *Sains Malaysiana*, vol. 46, no. 11, pp. 2019–2028, 2017.

[11] Y. B. Liu, *Study on the Deformation and Damage Rules of Gas-filled Coal Base on Meso-Mechanical Experiments*, Chongqing University, Chongqing, China, 2009.

[12] X. C. Li, B. S. Nie, J. W. Chen et al., "The experiment of different gas seepage in coal body under condition of different load," *Disaster Advances*, vol. 6, pp. 15–22, 2013.

[13] X. G. Liu, *Study on the Deformation and Failure Characteristics and the Permeation Behavior of Gas-saturated Coal*, China University of Mining and Technology, Xuzhou, China, 2013.

[14] R. S. Lv, *Research on Deformation-Seepage Characteristics and Mechanism of Gassy Coal under Load*, China University of Mining and Technology, Xuzhou, China, 2014.

[15] S. G. Cao, Y. Li, P. Guo, and Y. J. Bai, "Comparative research on permeability characteristics in complete stress-strain process of briquettes and coal samples," *Chinese Journal of Rock Mechanics and Engineering*, vol. 29, no. 5, pp. 899–906, 2010.

[16] D. Y. Li, M. Wang, B. B. Gao, and C. D. Su, "Research on permeability of large-sized coal sample in loading and unloading test," *Journal of Mining and Safety Engineering*, vol. 27, no. 1, pp. 121–125, 2010.

[17] Y. P. Cheng, H. Y. Liu, P. K. Guo, and R. K. Pan, "A theoretical model and evolution characteristic of mining-enhanced permeability deeper gassy coal seam," *Journal of China Coal Society*, vol. 39, no. 8, pp. 1650–1638, 2014.

[18] H. H. Liu and J. Rutqvist, "A new coal-permeability model: internal swelling stress and fracture-matrix interaction," *Transport in Porous Media*, vol. 82, no. 1, pp. 157–171, 2010.

[19] L. Wang, Z. Wang, S. Xu, W. Zhou, and J. Wu, "A field investigation of the deformation of protected coal and its application for CBM extraction in the Qinglong coalmine in China," *Journal of Natural Gas Science and Engineering*, vol. 27, pp. 367–373, 2015.

[20] C. Xu, Q. Fu, K. Wang, L. Yuan, and X. Zhang, "Effects of the loading methods on the damage-permeability aging characteristics of deep mining coal," *Journal of China University of Mining and Technology*, vol. 47, no. 1, pp. 197–205, 2018.

[21] S. G. Li, Y. Ding, T. J. Zhang, and G. Xu, "Experiment on permeability properties of coal samples with low permeability in complete stress-strain process," *Coal Safety*, vol. 6, pp. 5–8, 2013.

[22] Y. J. Yang, Y. Song, and S. J. Cheng, "Test study on permeability properties of coal specimen in complete stress-strain process," *Rock and Soil Mechanics*, vol. 28, no. 2, pp. 381–385, 2007.

[23] K. Y. Tian and R. L. Zhang, "Research on triaxial stress seepage experiment device loaded by high pressure water and negative pressure," *Rock and Soil Mechanics*, vol. 35, no. 21, pp. 3338–3344, 2014.

[24] R. K. Pan, Y. P. Cheng, J. Dong, and H. D. Chen, "Research on permeability characteristics of layered natural coal under different loading and unloading," *Journal of China Coal Society*, vol. 39, no. 3, pp. 473–477, 2014.

[25] G. R. Wang, D. J. Xue, H. L. Hao, and H. W. Zhou, "Study on permeability characteristics of coal rock in complete stress-strain process," *Journal of China Coal Society*, vol. 37, no. 1, pp. 107–112, 2012.

[26] C. R. Clarkson, C. L. Jordan, D. Ilk, and T. A. Blasingame, "Rate-transient analysis of 2-phase (gas + water) CBM wells," *Journal of Natural Gas Science and Engineering*, vol. 8, pp. 106–120, 2012.

[27] T. J. Zhang, S. G. Li, and Z. Q. Cheng, "Characteristics of micropores and their permeability characteristics of coal," *Journal of XIAN' University of Science and Technology*, vol. 28, no. 2, pp. 310–313, 2008.

[28] C. Zhang, S. H. Tu, and L. Zhang, "Study of stress sensitivity of coal samples with different mining damage in overlying strata," *Journal of China University of Mining and Technology*, vol. 47, no. 3, pp. 502–511, 2018.

[29] Z. G. Ma, X. X. Miu, Z. Q. Chen, and Y. S. Li, "Experimental study of permeability of broken coal," *Rock and Soil Mechanics*, vol. 30, no. 4, pp. 985–988, 2009.

[30] Z. Z. Wang, Q. L. Hou, and B. S. Yu, "Anisotropic characteristics of low-rank coal fractures in the Fukang mining area, China," *Fuel*, vol. 211, pp. 182–193, 2012.

[31] Y. Zhang, X. Xu, M. Lebedev, M. Sarmadivaleh, A. Barifcani, and S. Iglauer, "Multi-scale x-ray computed tomography analysis of coal microstructure and permeability changes as a function of effective stress," *International Journal of Coal Geology*, vol. 165, pp. 149–156, 2016.

[32] R. K. Pan, L. Wang, X. J. Chen, and H. D. Chen, "Study on permeability characteristics of unloading coal body and stress effect of microstructure," *Coal Science and Technology*, vol. 41, no. 7, pp. 75–78, 2013.

[33] J. Zhai, J. Wang, G. Lu, X. Qin, and W. Wang, "Permeability characteristics of remolded tectonically deformed coal and its influence factors," *Journal of Natural Gas Science and Engineering*, vol. 53, pp. 22–31, 2018.

[34] W. B. Han, G. Zhou, D. H. Gao et al., "Experimental analysis of the pore structure and fractal characteristicsof different metamorphic coal based on mercury intrusion-nitrogenadsorption porosimetry," *Powder Technology*, vol. 362, pp. 386–398, 2019.

[35] W. Han, G. Zhou, Q. Zhang, H. Pan, and D. Liu, "Experimental study on modification of physicochemical characteristics of acidified coal by surfactants and ionic liquids," *Fuel*, vol. 266, Article ID 116966, 2020.

[36] H. K. Ren, A. M. Wang, C. F. Li, and D. Y. Cao, "Study on porosity characteristics of low-rank coal reservoirs based on nuclear magnetic resonance technology," *Journal of Natural Gas Science and Engineering*, vol. 45, no. 4, pp. 143–148, 2017.

[37] Y. B. Yao and D. M. Liu, "Petrophysics and fluid properties characterizations of coalbed methane reservoir by using NMR relaxation time analysis," *Coal Science and Technology*, vol. 44, no. 6, pp. 14–22, 2016.

[38] S. B. Xie, Y. B. Yao, J. Y. Chen, and W. Yao, "Research of micro-pore structure in coal reservoir using low-field NMR," *Journal of China Coal Society*, vol. 40, no. 1, pp. 170–176, 2015.

[39] Y. B. Yao, D. M. Liu, Y. D. Cai, and J. Q. Li, "Fine quantitative characterization of pore cracks in coal based on NMR and X-CT," *Chinese Science Earth Science*, vol. 40, no. 11, pp. 1958–1607, 2010.